GEOLOGY | THE GEOLOGICAL SOCIETY OF AMERICA®

https://doi.org/10.1130/G45769.1

Manuscript received 31 October 2018
Revised manuscript received 14 January 2019
Manuscript accepted 10 February 2019

Published online 6 March 2019

A geomorphological assessment of wash-load sediment fluxes and floodplain sediment sinks along the lower Amazon River

Edward Park and Edgardo M. Latrubesse
Earth Observatory of Singapore and Asian School of the Environment, Nanyang Technological University, 637459 Singapore

ABSTRACT

We present the first spatiotemporal surface suspended sediment concentration (SSSC) analysis of the lower Amazon River, by combining geomorphological mapping, hydrosedimentological field investigations, and 15 years (2001–2015) of weekly averaged wash-load (fine sediment) fluxes at gauging stations estimated from field-calibrated remote-sensing models of SSSC. We found a downstream increase in the magnitude of sediment sinks, where the floodplain geomorphic style controls sediment trapping, and we conclude that the sediment net loss in the floodplain happens during the rising phase through seasonal hydrosedimentological connectivity. On average, 120 million tons per year of fine sediments are accumulated in the floodplain along 765 km of the lower Amazon River (from the confluence with the Madeira River to Monte Alegre city), making the lower Amazon River one of the most important fluvial sediment sinks among the world's axial rivers.

INTRODUCTION

The floodplains of the largest axial rivers can act as continental sedimentary sinks by storing sediment and preserving sediment archives in the geological record (Latrubesse, 2015). However, it remains challenging, both scientifically and methodologically, to understand "where" the sediments are stored in the alluvial reach, "how" the sediments are transferred to the sinks, "what" landforms result by channel-floodplain morphodynamics, and "how much" sediment is stored. Here, we intend to contribute to the understanding of these issues by studying Earth's largest axial river, the Amazon.

Dunne et al. (1998) quantified deposition rates in the channel and the floodplain between São Paulo do Olivença and Obidos, Brazil. Filizola and Guyot (2009) calculated the annual and seasonal deposition of suspended sediments from the Madeira River confluence to Obidos, and Mangiarotti et al. (2013) assessed wash-load storage between Itacoatiara and Obidos. Others have produced local sediment budgets in Curuai Lake (Fig. 1; Bourgoin et al., 2007; Rudorff et al., 2017) but obtained contrasting results.

Here, we updated and refined the lower Amazon floodplain sediment budgets using a new method that incorporates wash-load sediment fluxes and floodplain geomorphic styles (see the GSA Data Repository[1]). We analyzed the magnitude of sedimentation from Manacapuru to Monte Alegre (~1200 km) and identified the hotspots of sedimentation for muddy sediments (silt and clay), and we provide the first regional map of surface suspended sediment concentration (SSSC) of the lower Amazon River (Fig. 1).

Beyond the specific geoscientific interest, spatial understanding and quantification of channel-floodplain interactions in the Amazon are also environmentally relevant. The sediment regime of the Amazon River remains largely unregulated, but the construction of more than 200 dams has been proposed in the Amazon Basin. Consequently, any alteration of the sediment regime of the Amazon's floodplain, estuary, and sediment plume by dams is a major environmental concern (Latrubesse et al., 2017).

DATA AND METHODS

We used geomorphologic maps, hydrosedimentological field data, and daily discharges at eight gauging stations and collected SSSC samples, flow velocity data, and bathymetric information in the main channel, tributaries, and major floodplain lakes (Table DR1 in the Data Repository). Using field-calibrated remote-sensing models (based on 2944 images, 2740 SSSC samples from HYBAM [http://www.ore-hybam.org], and 121 SSSC samples we collected; Park and Latrubesse, 2014), we generated spatiotemporal SSSC maps along the lower Amazon River and estimated weekly averaged wash-load fluxes over 15 yr (2001–2015) at gauging stations (Table DR1; Fig. 1). Geomorphic mapping was performed using three classes: (1) impeded floodplain (IPF), (2) channel-dominated floodplain (CDF), and (3) levee complex (Latrubesse and Franzinelli, 2002; see also the Data Repository), and the area was divided in four reaches. Wash-load fluxes (Q_{wl}) at the gauging stations over 8 d intervals were calculated as:

$$Q_{wl} = SSSC_T \times Q_T \times k, \quad (1)$$

where $SSSC_T$ and Q_T denote SSSC and Q on a specific date T, while k is a conversion factor. The difference between influx and outflux from each reach at gauging stations for each period was computed, and the seasonal patterns of floodplain sediment storage and annual floodplain sediment budget for fine sediments were calculated. Then, the floodplain budget and geomorphic parameters were normalized to river lengths for comparison between the reaches. See Figure 1 for major floodplains and reaches 1–4. Migration rates (as channel-width per year, ch-w/yr) for the Amazon from Manacapuru to Monte Alegre over 30 yr (1985–2015) were obtained from Latrubesse et al. (2017; see the Data Repository).

RESULTS AND DISCUSSION

Downstream Patterns in Wash-Load Storage and Floodplain Geomorphology

Our assessment of floodplain deposition was based on wash-load fluxes at gauging stations as wash load was transferred to the floodplain

[1]GSA Data Repository item 2019135, methods, washload flux calculations, comparison of results with the seasonal pattern of suspended sediment discharge and floodplain sediment budget for the Amazon River reach in between Manacapuru and Obidos, Tables DR1–DR5, and Figures DR1–DR11, is available online at http://www.geosociety.org/datarepository/2019/, or on request from editing@geosociety.org.

CITATION: Park, E., and Latrubesse, E.M., 2019, A geomorphological assessment of wash-load sediment fluxes and floodplain sediment sinks along the lower Amazon River: Geology, v. 47, p. 403–406, https://doi.org/10.1130/G45769.1

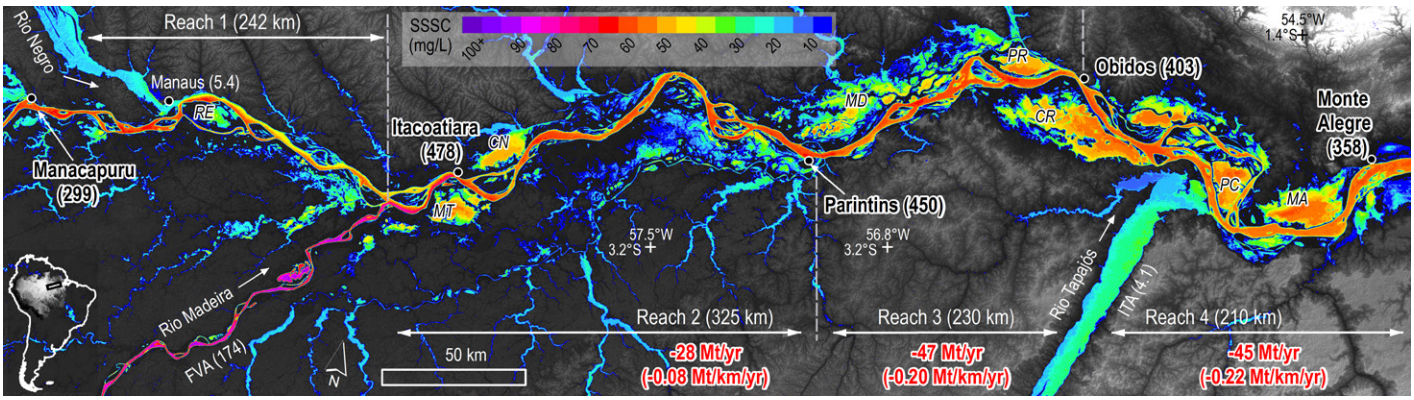

Figure 1. Averaged surface suspended sediment concentration (SSSC) map over December–February (2001–2015) of the Amazon River. Gauging stations and wash-load flux Q_{wl} (Mt/yr) are shown. Major floodplains: Rei (*RE*), Miratuba (*MT*), Canacari (*CN*), Madaba (*MD*), Paru (*PR*), Curuai (*CR*), Pacoval (*PC*), and Monte Alegre (*MA*). SSSC and bucket samples are marked as white and gray circles, respectively. Net floodplain sediment storage is in red. FVA—Fazenda Vista Alegre; ITA—Itaituba station on Tapajos River.

during floods, while the input of sandy sediments to the IPF, beyond the CDF, was very limited (see the Data Repository; Fig. 1).

Annual Q_{wl} values calculated at gauging stations Itacoatiara (*ITC*), Parintins (*PAR*), Obidos (*OBI*), and Monte Alegre (*MAL*) were 478, 450, 403, and 358 Mt, respectively, showing a decrease in wash-load discharge in the downstream direction (from reach 2 to reach 4; Fig. 1). Calculated per-kilometer floodplain sediment budgets were 0.08, 0.2, and 0.22 Mt/km/yr for reaches 2, 3, and 4, respectively, showing increasing sedimentation downstream. We identified the spatiotemporal distribution of SSSC over the mosaic of geomorphic units of the floodplain (Fig. 1). Our budget results and the distribution of the main sediment sinks have been persistent over a multidecadal scale, as inferred from the low channel migration rate along the lower Amazon River (0.01 ch-w/yr) and the geomorphologic characteristics of the IPF.

The floodplain in the lower Amazon extends over 1000 km in length and tens of kilometers in width (Fig. 1). The area of the CDF decreases from reaches 1 to 2 and remains small throughout reach 3 (Fig. 2B). Amazon River alluvial banks are composed of >80% of fine materials (silt and clay) and <20% of sands (Mertes et al., 1996). The high channel stability contributes to sustaining the large lateral lakes by limiting floodplain reworking by the main channel. However, the impounded water and flooded areas became larger in downstream directions, suggesting greater space for seasonal water and sediment storage (Fig. DR8). The largest areas of floodplain lakes are concentrated downstream of the Madeira River confluence (Sippel et al., 1992). The normalized areas of the IPF per unit river length for the four reaches also increase downstream (Fig. 2B). The IPF acts as a sink of gray-green muddy sediments at the millennial scale, as confirmed by ^{14}C dating (2.8 to ca. 1 ka) of organic sediments and logs at Careiro Island in reach 1 (Latrubesse and Franzinelli, 2002).

Loss of fine sediments in reach 1 is minimal, because high outcrops of old sedimentary rocks confine the left bank, and the confluence with the Negro River constrains the Amazon's muddy waters on the right bank (Park and Latrubesse, 2015). The development of the IPF floodplain in reach 1 is also limited and disconnected from the main channel by CDF levees.

Sediment storage increases in reaches 2–4. During the flood season, the IPF first receives water from the river through channelized flow initiated by levee breaching and through decadal-scale quasi-permanent floodplain channels, even before the river reaches bankfull stage. Floodplain channels connect the river to distal flood basins, generating splay-like deltas that progressively infill the depressions (lakes and ponds) of the IPF.

At bankfull stage, overbank dispersal becomes the dominant process. Mertes et al. (1996) showed that the freeboard at maximum flood between Parintins and Obidos is ~1 m. We characterized overbank flow potential by surveying the riverbank heights and found a downstream decrease in bank height (Fig. 2A). This implies an increase of susceptibility to overbank flooding and to floodplain wash-load influxes in reach 4. The magnitude and frequency of the overbank diffusion on the IPF vary among different reaches. They are mainly controlled by the bank height, and the heterogeneous distribution and complexity of the geomorphic mosaic of the

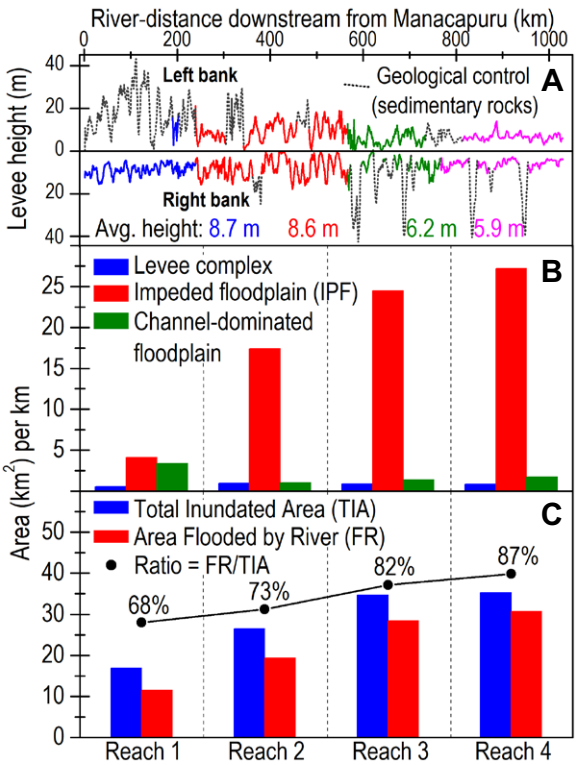

Figure 2. A: Bank height downstream along the Amazon River. B: Floodplain geomorphic unit composition. C: Total inundated area and areas flooded by river in floodplain, and ratio between them.

IPF (Table DR5). The large, shallow, and interconnected lakes and depressions of the IPF can be flooded by overbank waters and efficiently trap wash load, but the IPF can also be inundated with local sediment-free water sources (e.g., rainfall or surrounding drainage basins). Thus, we identified the lake areas directly influenced by sediment-laden river water that contributed to the floodplain sedimentation. For this, we decoupled the area flooded by the river (FR) from the total inundated area (TIA; Fig. 2C) by using SSSC maps (Fig. 1). The FR increases from reach 1 to 4, favoring sediment-laden water to spread over a wider area of the floodplain downstream. The ratio between FR and TIA increased downstream (from 68% for reach 1 to 87% for reach 4), showing that areal contribution of water sourced directly from the river out of the total inundated area also increased downstream. Although this planimetric analysis does not directly translate to volumetric information, it can be inferred that the river hydrology becomes more influential in controlling the floodplain inundation patterns and wash-load sediment transference downstream, where the floodplain is wider and incompletely fill by sediments.

Seasonal Storage of Sediment in the Floodplain and Budget

Meade et al. (1985) first claimed that storage in the lower Amazon River occurred during the rising stage and that partial resuspension of sediments occurred in the CDF. Dunne et al. (1998) also concluded that floodplain storage happened mainly during the rising stage and calculated a floodplain net sedimentation rate of 500 Mt/yr from the Peruvian border to Obidos. Filizola and Guyot (2009) estimated floodplain deposition of fine sediments from Manacapuru to Obidos to be 160 Mt/yr, identifying major loss of wash load between a longer period spanning from March to October. Our results indicate that wash-load net loss should include only the rising phase, when the river makes hydrologic connections to the floodplain (Fig. 3B; Park and Latrubesse, 2017). Bourgoin et al. (2007) and Rudorff et al. (2017) also concluded that local net sedimentation in the Curuai floodplain is positive only during the rising phase.

We investigated the seasonal patterns of floodplain wash-load loss, using the same reach, from Manacapuru to Obidos (reaches 1–3), by subtracting the combined mean monthly Q_{wl} fluxes upstream (i.e., $Q_{wlMAN} + Q_{wlFVA} + Q_{wlMAO}$ [Man—Manacapuru; FVA—Fazenda Vista Alegre; MAO—Manaus]) from the mean monthly Q_{wl} curve at Obidos (Q_{wlOBI}; Fig. 3A). Net sedimentation in the floodplain spans from September to May, with the highest rate of sedimentation in January (~19.7 Mt), when Q_{wlMAN} is the highest of the year. A high rate of wash-load loss is maintained until March, when Q_{wl} at both *FVA* and *OBI* are at the peak, and then gradually decreases. In June–July, when the Amazon is at flood peak stage, the wash-load budget is balanced (Fig. 3B). From March-April to October, Q and Q_{wl} at *FVA* from the Madeira River decrease, and in June-July, when the Amazon's water level peaks, the lower Madeira River experiences a significant backwater effect from the Amazon (Fig. DR4; Meade et al., 1991). Thus, from July to October, the Q_{wl} contribution of the Madeira is the lowest (3 Mt/mo; Fig. 3A). Correspondingly, during the falling phase, the Amazon River presents low-magnitude net gain of wash load in July and August (3.6 Mt/yr) but remains close to equilibrium in June and September.

Overall, the mean annual net loss of wash load (deposition) from Manacapuru to Obidos (reaches 1–3) is estimated to be 76 Mt (Fig. 3B).

Averaged sedimentation rates for long reaches of the Amazon range from ~0.12 to 0.41 Mt/km/yr (Dunne et al., 1998; Mangiarotti et al., 2013). However, interpolation of sediment storage per reach can hide local variation in the rates of floodplain deposition, and the geomorphic heterogeneity of the floodplain prevents both regular distribution of channelized connections and even distribution of overbank dispersion of sediments. The SSSC in Figure 1 is a direct indicator of the distribution and extent of sediment sinks during the rising stage (December–February). Our mapping detected a downstream trend of larger impounded water areas in the floodplain with a higher SSSC (from reaches 1 to 4), indicating that wash load is transferred during the rising stage several kilometers toward the inner parts of the IPF, while the area of the CDF proportionally decreases downstream.

Mertes (1994) concluded that a peirheic zone of diluted river water covers large areas of the floodplain around Manacapuru (reach 1), and that the high rate of suspended sediment transferred during floods (4–18 T/km/d of silts) should settle in the proximal floodplain (~700 m from the banks). This lower transference of sediments into the water-saturated area of the IPF in reach 1 was also detected in our SSSC mapping (Fig. 1). It happens because the well-developed CDF in the Solimões River constrains flooding and provides limited channel-floodplain connectivity toward the IPF (Fig. 2B). Thus, the coarse suspended sediments are deposited in the proximal narrow belt of the CDF, which is architecturally composed of "in-channel" landforms and sediments, such as confined levee complexes, sinuous branches, scrolls, and islands (Latrubesse and Franzinelli, 2002; Mertes, 1997). It is also related to the geomorphologic maturity (sediment infill) of the IPF. Levees in reach 1 are above the mean annual flood level and constrain the lateral spatial availability for dispersion and accommodation of sediments in the floodplain (Fig. 2A).

While the average SSSC (December–February) of the floodplain in reaches 1 and 2 rarely increase above 40 mg/L, the SSSCs of the floodplain lakes along reaches 3 and 4 were generally above 60 mg/L (Fig. 1). Trapping efficiency in the floodplain during floods in reaches 2–4 is significant, and the water velocity (in the major floodplain lakes and inlet-outlets) is commonly below a critical velocity of ~0.15 m/s to null, favoring the sedimentation of fine sediments (Mangini et al., 2015; see also Figure DR9 and Table DR4).

The capacity of annual storage is still low in reach 2, with a trapping rate averaged at 28 Mt/yr (0.08 Mt/km/yr). The heights of average levees and alluvial banks gradually decrease toward reaches 3 and 4 (Fig. 2A), and we calculated 47 and 45 Mt/yr, and 0.20 and 0.22 Mt/km of annual net sedimentation and linear rate of sedimentation, respectively. Our analyses for the total studied length of 765 km (reaches 2–4) indicate that the lower Amazon River is storing ~120 Mt/yr of fine sediments in the floodplain.

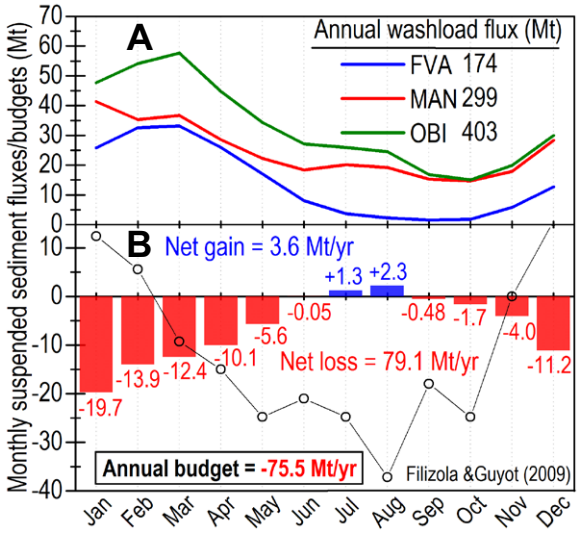

Figure 3. A: Monthly wash-load flux, Q_{wl}, at *FVA*, *MAN* (FVA—Fazenda Vista Alegre; Man—Manacapuru), and Obidos (*OBI*) calculated over 15 yr (2001–2015). B: Monthly floodplain sediment budgets between Madeira River confluence and Obidos. Budget by Filizola and Guyot (2009) is also shown.

SUMMARY

We generated the first SSSC map for 1200 km of the lower Amazon River, estimated net floodplain deposition of fine sediments, identified the distribution of wash-load sediment sinks, addressed how they are related to the floodplain geomorphology on a reach scale, and provided new insights into the seasonal floodplain storage patterns. Fine sediment trapping efficiency varies with channel and floodplain style, and it is mainly related to the "impeded floodplain (IPF)" geomorphological unit, which contains large rounded lakes and is characterized by widespread overbank flooding.

Because of the changes in the floodplain geomorphic style, the magnitude of sediment sinks increases downstream. The main factors are (1) a wide valley with a stable anabranching channel confined by levees that do not rework the floodplain significantly; (2) decreasing bank height downstream that favors larger magnitudes and more frequent overbank diffusion; and (3) space accommodation from a wider water-saturated IPF with lentic condition that potentiates sediment deposition in the distal floodplain. We conclude that the net loss to the floodplain occurs during the rising phase, when the sediments are transferred to the floodplain through hydrogeomorphologic connections. On average, the annual accumulation of wash load in the floodplain along 765 km, from the Madeira River confluence to Monte Alegre, is 120 Mt of fine sediment, making the lower Amazon River one of the most crucial fluvial sediment sinks of the planet in terms of axial rivers.

ACKNOWLEDGMENTS

We acknowledge the National Science Foundation (NSF) Doctoral Dissertation Research Improvement award (1558446), NSF Frontiers in Earth System Dynamics (1338694) grant, Earth Observatory of Singapore (EOS), and SO-HYBAM (http://www.ore-hybam.org) for the gauging station data. We appreciate J. Stevaux, M. Bayer, L. Santos, S. Aquino, and A. Slitine for their assistance in field and laboratory work, and the constructive comments by T. Dunne and two anonymous reviewers.

REFERENCES CITED

Bourgoin, L.M., Bonnet, M.-P., Martinez, J.-M., Kosuth, P., Cochonneau, G., Moreira-Turcq, P., Guyot, J.-L., Vauchel, P., Filizola, N., and Seyler, P., 2007, Temporal dynamics of water and sediment exchanges between the Curuaí floodplain and the Amazon River, Brazil: Journal of Hydrology (Amsterdam), v. 335, p. 140–156, https://doi.org/10.1016/j.jhydrol.2006.11.023.

Dunne, T., Mertes, L.A.K., Meade, R.H., Richey, J.E., and Forsberg, B.R., 1998, Exchanges of sediment between the flood plain and channel of the Amazon River in Brazil: Geological Society of America Bulletin, v. 110, p. 450–467, https://doi.org/10.1130/0016-7606(1998)110<0450:eosbtf>2.3.co;2

Filizola, N., and Guyot, J.L., 2009, Suspended sediment yields in the Amazon Basin: An assessment using the Brazilian national data set: Hydrological Processes, v. 23, p. 3207–3215, https://doi.org/10.1002/hyp.7394.

Latrubesse, E.M., 2015, Large rivers, megafans and other Quaternary avulsive fluvial systems: A potential "who's who" in the geological record: Earth-Science Reviews, v. 146, p. 1–30, https://doi.org/10.1016/j.earscirev.2015.03.004.

Latrubesse, E.M., and Franzinelli, E., 2002, The Holocene alluvial plain of the middle Amazon River, Brazil: Geomorphology, v. 44, p. 241–257, https://doi.org/10.1016/S0169-555X(01)00177-5.

Latrubesse, E.M., et al., 2017, Damming the rivers of the Amazon Basin: Nature, v. 546, p. 363–369, https://doi.org/10.1038/nature22333.

Mangiarotti, S., Martinez, J.M., Bonnet, M.P., Buarque, D.C., Filizola, N., and Mazzega, P., 2013, Discharge and suspended sediment flux estimated along the mainstream of the Amazon and the Madeira Rivers (from in situ and MODIS satellite data): International Journal of Applied Earth Observation and Geoinformation, v. 21, p. 341–355, https://doi.org/10.1016/j.jag.2012.07.015.

Mangini, S.P., Prendes, H.H., Amsler, M.L., and Huespe, J., 2015, Importancia de la floculación en la sedimentación de la carga de lavado en ambientes del río Paraná, Argentina: Instituto Mexicano de Tecnología del Agua Inicio, v. 18, p. 55–69.

Meade, R.H., Dunne, T., Richey, J.E., Santos, U.M., and Salati, E., 1985, Storage and remobilization of suspended sediment in the lower Amazon River of Brazil: Science, v. 228, p. 488–490, https://doi.org/10.1126/science.228.4698.488.

Meade, R.H., Rayol, J.M., Daconceicao, S.C., and Natividade, J.R.G., 1991, Backwater effects in the Amazon River Basin of Brazil: Environmental Geology and Water Sciences, v. 18, p. 105–114, https://doi.org/10.1007/BF01704664.

Mertes, L.A., 1994, Rates of flood-plain sedimentation on the central Amazon River: Geology, v. 22, p. 171–174, https://doi.org/10.1130/0091-7613(1994)022<0171:ROFPSO>2.3.CO;2.

Mertes, L.A., 1997, Documentation and significance of the perirheic zone on inundated floodplains: Water Resources Research, v. 33, p. 1749–1762, https://doi.org/10.1029/97WR00658.

Mertes, L.A., Dunne, T., and Martinelli, L.A., 1996, Channel-floodplain geomorphology along the Solimões-Amazon River, Brazil: Geological Society of America Bulletin, v. 108, p. 1089–1107, https://doi.org/10.1130/0016-7606(1996)108<1089:CFGATS>2.3.CO;2.

Park, E., and Latrubesse, E.M., 2014, Modeling suspended sediment distribution patterns of the Amazon River using MODIS data: Remote Sensing of Environment, v. 147, p. 232–242, https://doi.org/10.1016/j.rse.2014.03.013.

Park, E., and Latrubesse, E.M., 2015, Surface water types and sediment distribution patterns at the confluence of mega rivers: The Solimões-Amazon and Negro Rivers junction: Water Resources Research, v. 51, p. 6197–6213, https://doi.org/10.1002/2014WR016757.

Park, E., and Latrubesse, E.M., 2017, The hydrogeomorphologic complexity of the lower Amazon River floodplain and hydrological connectivity assessed by remote sensing and field control: Remote Sensing of Environment, v. 198, p. 321–332, https://doi.org/10.1016/j.rse.2017.06.021.

Rudorff, C. M., Dunne, T., and Melack, J. M., 2017, Recent increase of river-floodplain suspended sediment exchange in a reach of the lower Amazon River: Earth Surface Processes and Landforms, v. 43, p. 322–332, https://doi.org/10.1002/esp.4247.

Sippel, S., Hamilton, S., and Melack, J., 1992, Inundation area and morphometry of lakes on the Amazon River floodplain, Brazil: Archiv für Hydrobiologie, v. 123, p. 385–400.

Printed in USA